Molecular Crystals and Liquid Crystals Science and Technology. Section A. Molecular Crystals and Liquid Crystals

Publication details, including instructions for authors and subscription information:
http://www.tandfonline.com/loi/gmcl19

Nonlinear Effects in Liquid Crystal Waveguides: Theory and Experiment

Giancarlo Abbate [a] , Francesca Castaldo [a] & Luca De Stefano [a]

[a] INFM, Dipartimento di Scienze Fisiche, Università di Napoli, Pad. 20, Mostra d'Oltremare, 80125, Napoli, Italy

Version of record first published: 24 Sep 2006.

To cite this article: Giancarlo Abbate , Francesca Castaldo & Luca De Stefano (1996): Nonlinear Effects in Liquid Crystal Waveguides: Theory and Experiment, Molecular Crystals and Liquid Crystals Science and Technology. Section A. Molecular Crystals and Liquid Crystals, 282:1, 269-285

To link to this article: http://dx.doi.org/10.1080/10587259608037581

Mol. Cryst. Liq. Cryst., 1996, Vol. 282, pp. 269–285
Reprints available directly from the publisher
Photocopying permitted by license only

NONLINEAR EFFECTS IN LIQUID CRYSTAL WAVEGUIDES: THEORY AND EXPERIMENT

GIANCARLO ABBATE, FRANCESCA CASTALDO, LUCA DE STEFANO

INFM, Dipartimento di Scienze Fisiche, Università di Napoli, Pad.20, Mostra d'Oltremare, 80125, Napoli, Italy

Abstract A theoretical and experimental study of the nonlinear properties of a waveguide, whose core is filled by a nematic L.C., is presented.
Hybrid, homeotropic and planar alignments at the waveguide walls we considered in the strong anchoring approximation.
In the case of the homeotropic alignment with negative optical torque a spatial splitting of the guided field is expected similar to the one already observed in a L.C. electro-optic device.

INTRODUCTION

The use of Liquid Crystals (LC) in guiding devices such as planar waveguides and cylindrical fibers has been reported since the 70's.[1,2] The wide variety of mechanical and optical properties including viscosity and refractive indices, and, overall, the strong response to weak external fields (magnetic, electric and optical) render LC particularly attractive for the realization of electro-optical or all-optical guided devices. The slow response time and the high scattering losses however have greatly limited the use of the proposed devices in practical applications. Nevertheless, in the last two or three years, the interest in the LC guided devices has been renewed both from a fundamental point of view and from the applicative one.[3–7] In particular, all-optical and nonlinear LC devices could be of great interest in guided optics, at least for applications not requiring fast responses. A theoretical understanding and an experimental study of some model geometries is the first

step for a wider diffusion of the applications of LC guided devices. In this paper, a brief review of recently obtained results in the study of nonlinear effects in nematic LC waveguides is presented. Different geometries has been considered both theoretically and experimentally and for one of them very new, although preliminary, results are reported.

HYBRID ALIGNED NEMATIC

The first geometry we studied is a planar waveguide whose core is an HAN (Hybrid Aligned Nematic) cell. The scheme is presented in the insert of Figure 1. We choose the HAN geometry in order to avoid the occurrence of any threshold in

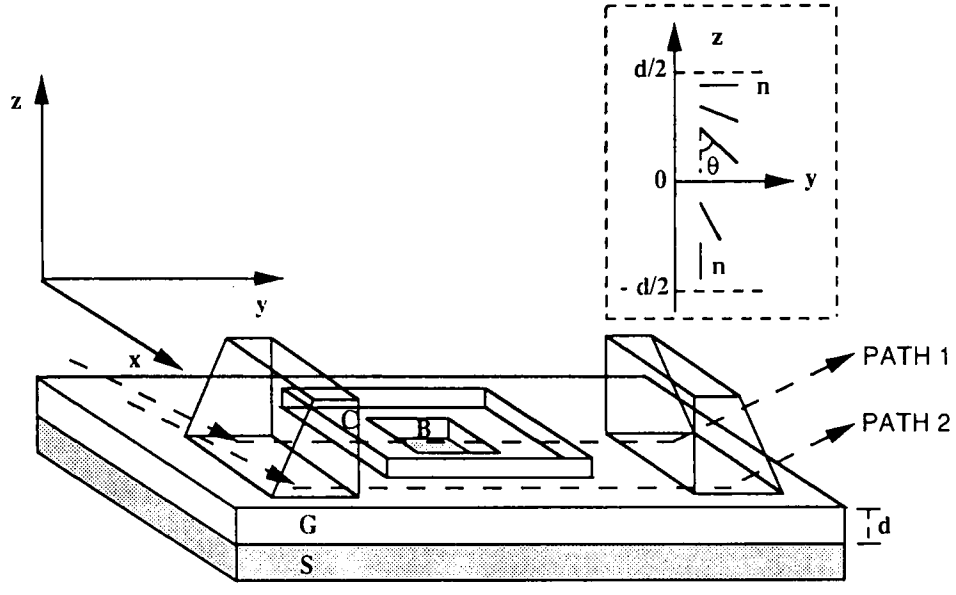

FIGURE 1 Scheme of the used planar waveguide with basin containing liquid crystal. G:Guide; S:Substrate; B:Basin; C:Cover; d=3.8μm waveguide thickness and basin depth; **n**: molecular director. Path 2: propagation in the linear glass waveguide. Path 1: propagation in the nonlinear LC waveguide.

the optical reorientation of the nematic director so that nonlinear effects are more

easily seen. The cover and the substrate of the guide are two identical glass plates, whose refractive index has been chosen lower than the ordinary refractive index of the LC in order to assure the guiding condition of a TM mode. The propagation of an optical field inside such a waveguide is a nonlinear problem and requires the simultaneous solution of Maxwell's equations for the light and the torque balance equation for the medium. The nonlinear coupling arises from the fact that an optical torque is acting on the medium determining its steady configuration and the configuration of the medium influences the light field propagation. We have presented elsewhere[8] a quite general approach to this problem in the case of plane wave and neglecting scattering inside the medium. In the case of a TM polarized light wave ($\mathbf{H} \equiv (H_x, 0, 0)$, $\mathbf{E} \equiv (0, E_y, E_z)$) propagating in the LC filled core of the waveguide the problem is greatly simplified and its solution can be afforded by suitable numerical technique. We get the following set of differential equations:

$$\begin{aligned} &\varepsilon_{33}^2 \quad R'' + \varepsilon_{33}\varepsilon_{33}' R' + k_0^2 \varepsilon_o \varepsilon_e (\varepsilon_{33} - \beta^2) R = 0 \\ &k_{33} \quad [(1 - k\sin^2\theta)\theta'' - k\sin\theta\cos\theta(\theta')^2] - \frac{\varepsilon_{23}}{8\pi}\left[\frac{\beta^2 R^2}{\varepsilon_{33}^2} - \frac{(R')^2}{k_o^2 \varepsilon_o \varepsilon_e}\right] = 0 \end{aligned} \qquad (1)$$

In these eqs. $R(z)$ is the field amplitude, defined by:

$$H_x(y, z, t) = R(z) e^{i\phi(z)} e^{i(k_o \beta y - \omega t)}$$

where $k_o = \omega/c$, ω being the optical frequency, β is the guided mode propagation constant, $k = 1 - \frac{k_{11}}{k_{33}}$ where k_{11} and k_{33} are the LC elastic constants; $\varepsilon_o = n_o^2$, $\varepsilon_e = n_e^2$, $\varepsilon_{23} = \varepsilon_a \sin\theta\cos\theta$, $\varepsilon_{33} = \varepsilon_o + \varepsilon_a \cos^2\theta$ with $\varepsilon_a = n_e^2 - n_o^2$, n_e and n_o being the extraordinary and ordinary refractive indices of the LC respectively; and θ is the angle which the director $\mathbf{n} = (0, \sin\theta, \cos\theta)$ forms with the stratification direction z.

The set (1) must be completed with proper boundary conditions, which in our case read:

$$\begin{aligned} R'\left(-\frac{L}{2}\right) &= \frac{n_o^2}{n_p^2}\sqrt{\beta^2 - n_p^2} k_o R\left(-\frac{L}{2}\right) \\ R'\left(\frac{L}{2}\right) &= -\frac{n_e^2}{n_p^2}\sqrt{\beta^2 - n_p^2} k_o R\left(\frac{L}{2}\right) \end{aligned}$$

for the fields, and

$$\theta\left(-\frac{L}{2}\right) = 0$$
$$\theta\left(\frac{L}{2}\right) = \frac{\pi}{2}$$

for the medium, where L is the thickness of the waveguide core.

Thus, we are dealing with a nonlinear eigenvalue problem, the eigenvalue being the nonlinear propagation constant β. This problem has been solved with an expressly made numerical technique based on the continuation method.[9] We made a set of numerical simulation using the material parameters of E7, a commercial LC mixture, from BDH catalog, which is one of the materials we actually used in the experiments. In Figure 2 some of the obtained results are summarized. Figure 2a shows the nonlinear propagation constant β vs. the guided power per unit length (p.u.l.) for three different eigensolutions corresponding to the first three modes of the unperturbed guide. Figures 2b, 2c and 2d refer only to the first eigensolution and show the spatial distribution inside the waveguide of the director distortion, of the effective index and of the optical field amplitude, respectively. The power p.u.l. is the parameter. From these figures, in particular from Fig. 2d, we clearly see the tendency of the guided light to propagate along the high index side of the waveguide. When the guided power is increased, however, the high index region enlarges, thus pushing the field towards the middle of the cell. The absence of threshold in the HAN cell leads to significant nonlinear effects even for low guided power and to a rapid saturation for high power.

The biggest problem in the realization of an experimental setup to observe the above described effects is the achievement of a reasonable coupling of the light into the LC waveguide. We have decided to directly couple the light from another waveguide, a linear glass waveguide, exactly faced to our LC cell. The light decoupling was obtained in the same way. For this purpose, we have designed* the structure shown in Figure 1. It is a dielectric multimode waveguide, realized by sputtering glass on glass, having refractive indices of core and substrate n_g=1.555

*This device has been realized at IROE of CNR in Florence (Italy) by the group of Dr. G.C.Righini.

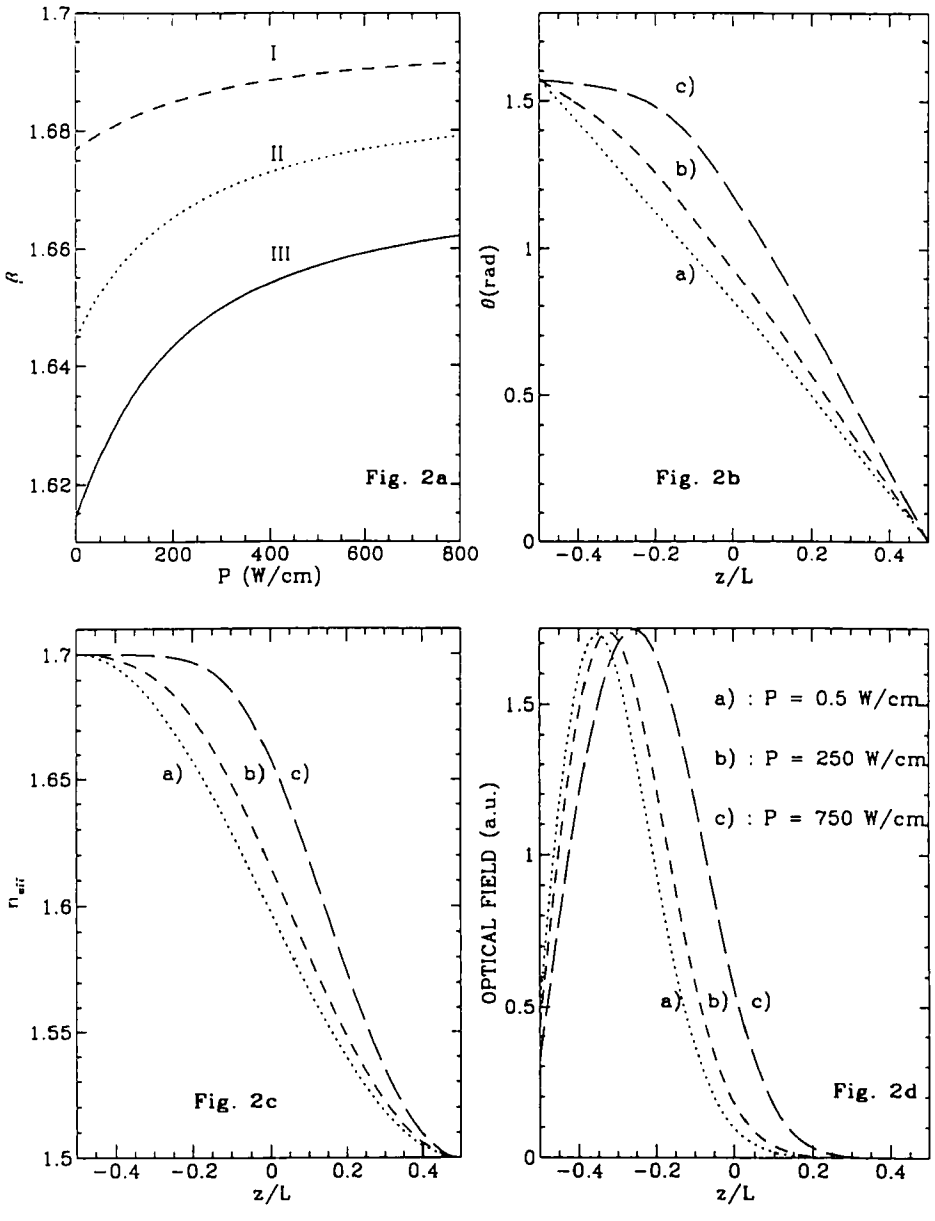

FIGURE 2 TM wave propagation in an HAN LC waveguide: numerical results. The propagation constant β for the first three modes vs. the power per unit length (2a). The director distortion θ (2b), the effective index (2c) and the field amplitude (2d) of the first mode vs. stratification coordinate for different guided powers.

and n_p=1.520, respectively, at wavelength λ=514.5 nm. A basin, to be filled with the nematic LC, 1 mm long, 10 mm wide and 3.8 μm depth as the thickness of the glass waveguide core, was then dug into it. We have obtained an HAN cell forcing homeotropic anchoring to the basin bottom and planar anchoring to the glass cover with proper surfactants. The light beam, coupled by means of high index prism, can propagate along either path 1 (Figure 1), i.e. the series of three directly coupled waveguides, linear glass + nonlinear LC + linear glass, or path 2, i.e. just one linear glass waveguide. We will call, in the following, the three waveguides along path 1, IWG (Input WaveGuide), LCWG (Liquid Crystal WaveGuide) and OWG (Output WaveGuide). The light beam is finally decoupled by means of a second high index prism and projected onto a screen or sent into a power meter. The comparison of the results between path 1 and path 2, in the same experimental conditions, allows to avoid spurious effects, as the effects due to the heating of the air gap between the coupling prism and the IWG. Results are summarized in Figure 3 in terms of the power distribution within the first three modes of the OWG. A nonlinear change in the field amplitude profile in the LCWG leads to a different coupling with the modes of the OWG, which results in different power distribution among them, when the total guided power is increased. The fractions $R_m = \frac{P_m^{out}}{\sum_m P_m^{out}}$ of the output power in the m-th mode ($m \in \{1,2,3\}$) are independent of the power p.u.l. when the light propagates along path 2 (Fig. 3a), while they suffer dramatic variations when the light propagates along path 1, as shown in Fig. 3b. As discussed above, at low guided power the maximum of the amplitude profile in the LCWG is from one side of the cell, thus the best coupling is achieved with the second mode of the OWG. At higher power, the pushing of this maximum towards the middle of the cell leads to best coupling with the first mode of the OWG. Further increase of the guided power doesn't change anymore the power distribution among the modes, indicating that saturation has been reached. To render this interpretation of the experimental results more quantitative, we performed a calculation of the coupling coefficients by means of the overlap integrals theory.[10] In this calculations

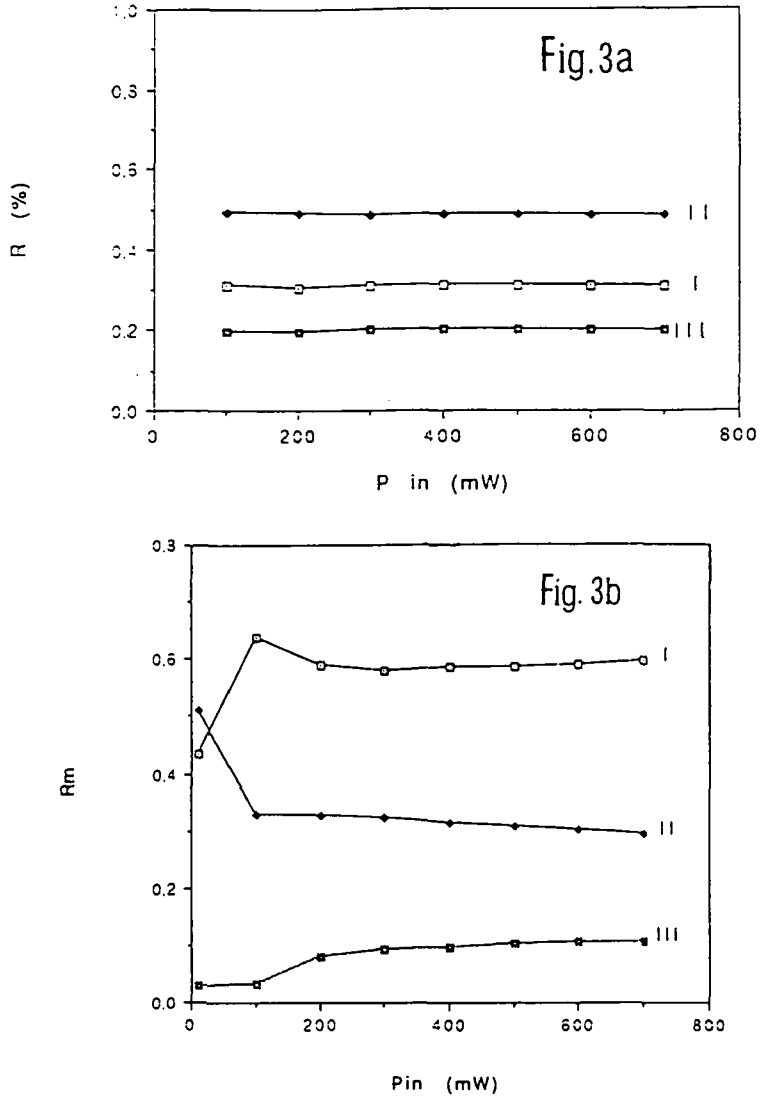

FIGURE 3 The distribution of the output power fraction R_m on the first three modes of the OWG as a function of the input power, for a TM wave propagating along path 2 (3a) and along path 1 (3b).

we assumed plane wave and we neglected reflection effects. First, we obtained for the coupling between IWG and LCWG, that each of the first three modes of IWG transfers 99% of the carried power into the first mode of the unperturbed LCWG. We may then retain only the first nonlinear solution in the LCWG. The power fraction R_m coupled by the last to the three modes of the OWG is shown in Figure 4 vs. the guided power p.u.l.. The values of $R_m(0)$ at very low total power have been adjusted to fit the experimental values. The agreement between experiment and theory is quite satisfactory.

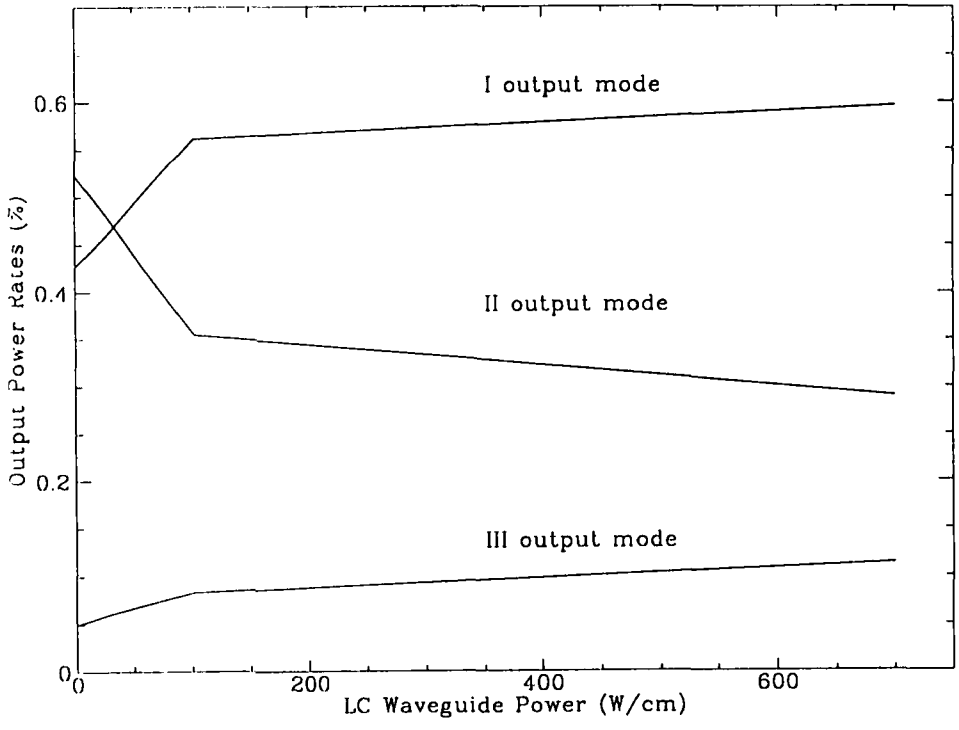

FIGURE 4 Theoretical distribution of the output power fraction R_m on the first three modes vs. the guided power, for a TM polarized light wave in the HAN LCWG.

PLANAR ALIGNED NEMATIC

The nonlinear propagation of a laser beam in a LC sample strongly depends the anchoring conditions at the boundaries. Unlike the HAN case, the existence of a power p.u.l. threshold for the molecular reorientation is expected, by symmetry consideration, in the cases of homogeneous planar and homeotropic alignment of the LCWG, in analogy with the Optical Fréedericksz Transition (OFT) at normal incidence. Let us consider a symmetric LCWG, whose core is a nematic liquid crystal cell, 2μm thick, planarly aligned with the easy-axis along the y direction.[11] The cover and the substrate are two identical glass plates, with $n_g < n_o$. For a TM wave, the propagation equations are still eqs. (1),but with the new boundary conditions:

$$R'\left(-\frac{L}{2}\right) = \frac{n_e^2}{n_p^2}\sqrt{\beta^2 - n_p^2}k_o R\left(-\frac{L}{2}\right)$$

$$R'\left(\frac{L}{2}\right) = -\frac{n_e^2}{n_p^2}\sqrt{\beta^2 - n_p^2}k_o R\left(\frac{L}{2}\right)$$

for the fields, and

$$\theta\left(-\frac{L}{2}\right) = \frac{\pi}{2}$$

$$\theta\left(\frac{L}{2}\right) = \frac{\pi}{2}$$

for the medium.

These boundary conditions lead to uniform distribution of the molecular director and to a symmetric, bell shaped, field amplitude profile inside the LCWG. The uniform distribution is stable at low guided power.

With our numerical technique we get the results shown in Figure 5. From Fig. 5a, we see that the propagation constant of each eigensolution remain fixed to the value corresponding to the unperturbed sample, until a critical guided power p.u.l. is reached. Unlike the standard OFT, which is generally second order, the transition in our LCWG can be first order and accompanied by hysteresis. The order of the transition is found to be dependent on the guided mode and on the waveguide thickness: for very thin guides no first-order transition occurs, while thicker is the guide larger is the number of modes exhibiting first-order transition. In the insert of Fig. 5a the presence of a bistable loop for the first mode

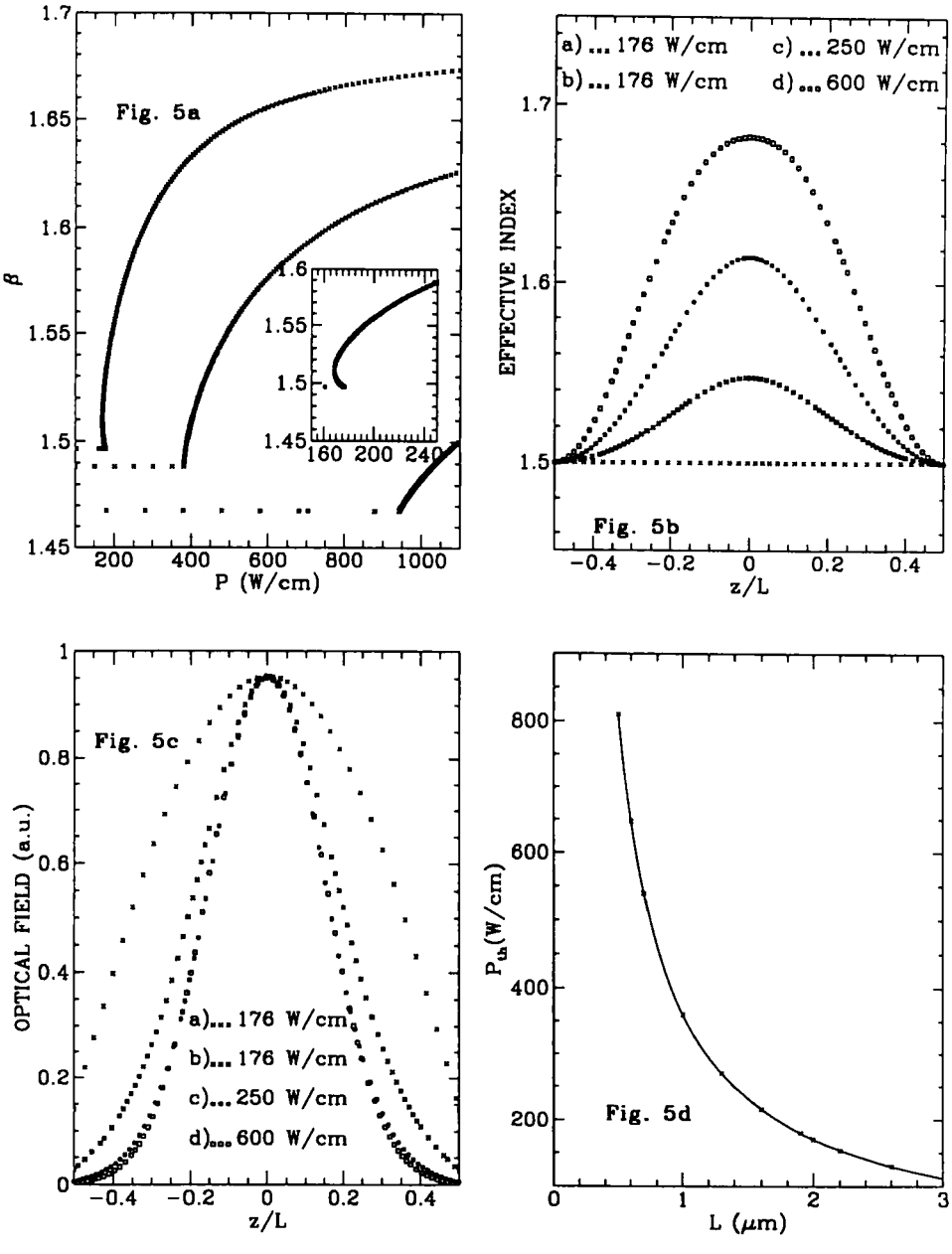

FIGURE 5 Theoretical results for a TM-wave in a planar aligned nematic LCWG. The propagation constant for the first three modes vs. the power per unit length (5a); the insert shows a magnification of the bistable region for the first mode. The spatial distribution inside the waveguide of the effective index (5b) and the field amplitude of the first mode (5c) for different guided powers. The reorientation threshold power p.u.l. vs. the core thickness (5d).

is made evident. This intrinsic optical bistability phenomenon is to be ascribed to the evolution of the field amplitude profile for increasing power, shown in Fig. 5b: as the power is increased above the threshold value the effective refractive index seen by the propagating wave, grows up in the middle of the film, see Fig. 5c. This causes a self-confinement of the beam and a consequent local increasing of the intensity. When the input power is decreased, the guided power concentrated at the waveguide center gives an optical torque strong enough to sustain the molecular reorientation even at guided power lower than the threshold value, yielding hysteresis. The self trapping effect depends physically on the strength of the anchoring forces and so, on the LC sample thickness. We computed the threshold power of the first mode as a function of the waveguide thickness. Up to 1μm, the power required to induce reorientation is far below $1kW/cm$, a value that can be easily obtained with a commercial c. w. laser. In Fig. 5d it is shown that the plot is well fitted by $1/L$ power low. This kind of scaling corresponds to the $1/L^2$ scaling of local intensity, as in the case of the OFT.

The experiment for a planarly aligned LCWG is being performed with the same device of Fig. 1, with proper change in the surfaces coating to ensure planar anchoring. The detected output signals are the same as in of the previous section. Till now, we were successful in observing a power threshold value below which the behavior of the LCWG is linear and above which it becomes drastically nonlinear. In Figure 6, the output power from the first mode of the OWG is plotted vs. the total guided power in the LCWG. The observed threshold value is in fairly agreement with the numerical expectation.

DYE-DOPED NEMATIC WITH HOMEOTROPIC ALIGNMENT

Recently, it has been discovered that inserting small amount, less than 1% w/w, of some absorbing dyes, greatly enhances the nonlinear optical response of the mixture, without increasing the response time. This is the so called Jánossy effect.[12] Although a complete model of this effect is not yet available, analysis of the experimental data suggests that the expression of the optical torque is still valid apart

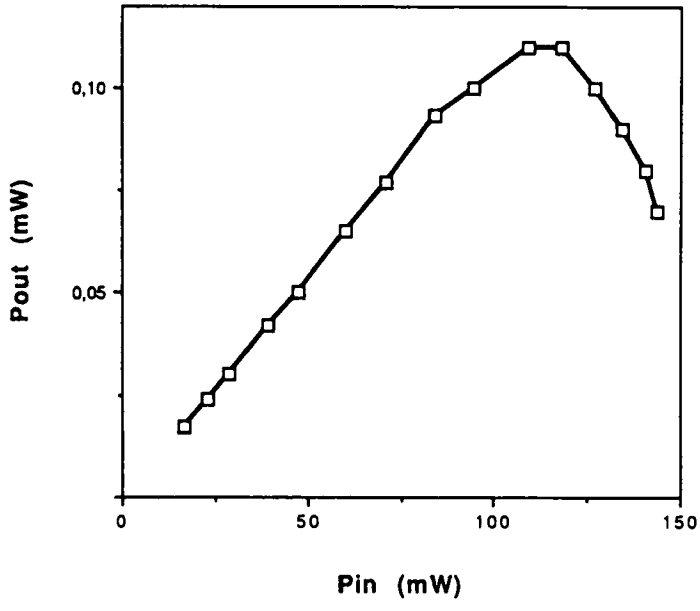

FIGURE 6 The measured output power on the first mode of the OWG vs. the input power.

from a coefficient η in front of the dielectric anisotropy ε_a:[13]

$$\tau_o = \frac{\eta \varepsilon_a}{4\pi} < (\mathbf{n} \cdot \mathbf{E})(\mathbf{n} \times \mathbf{E}) > \tag{2}$$

The numerical value of η depends on the dye, on the LC, on the concentration and on the wavelength and can be as large as 100 and both positive and negative. Let us consider a symmetrical LCWG with homeotropic anchoring at the walls. From eq. (2) it can be shown that for a TM guided wave no molecular reorientation is possible if η is positive, since the electric field of the light $\mathbf{E}$ is parallel to the nematic director $\mathbf{n}$, but if η is negative, an optical torque can arise above a proper threshold. Eqs. (1) must be modified in order to take into account the η factor and the new boundary conditions, that now read:

$$R'\left(-\frac{L}{2}\right) = \frac{n_o^2}{n_p^2}\sqrt{\beta^2 - n_p^2 k_o} R\left(-\frac{L}{2}\right)$$

$$R'\left(\frac{L}{2}\right) = -\frac{n_o^2}{n_p^2}\sqrt{\beta^2 - n_p^2 k_o} R\left(\frac{L}{2}\right)$$

for the fields, and

$$\theta\left(-\frac{L}{2}\right) = 0$$
$$\theta\left(\frac{L}{2}\right) = 0$$

for the director.

The numerical results obtained are summarized in Figure 7. In Fig. 7a the nonlinear propagation constant β is shown vs. the guided power p.u.l. for the first two eigensolutions. These solutions coalesce at some power value, indicating a degeneration also in the module of the field profiles. The effective refractive index and the field amplitude of the first eigensolution inside the LCWG are plotted in Fig. 7b and 7c, respectively, for three different power p.u.l. values. Due to the induced molecular reorientation above the threshold the effective index decreases in the middle of the cell while it remains higher at the cell boundaries because of the anchoring conditions. For this reason, the optical field is pushed towards the two sides of the waveguide, assuming a two-peaks symmetric profile. The field distribution of this first mode solution is then more and more similar to that of the second mode, apart from a phase factor: the moduli, indeed, become identical for the power p.u.l value, where the β's coalesce. We get a nonlinear spatial splitting of the guided beam which is more effective at higher power and which can lead to two spatially separated output beams. This effect appears very attractive to envisage useful integrated optics devices, and even more if we consider than the η factor enhancing the optical torque reduces the power needed to observe the nonlinear behavior. The plot of the threshold power p.u.l. vs. η is reported in Figure 7d. This nonlinear device is in course of realization. In a previous work,[14] we have realized a linear electro-optical device completely analogous to it. In this device the director reorientation is achieved by means of an externally applied static electric field. The results obtained are shown in Figure 8 (8a computed and 8b measured), where the optical field intensity inside the LCWG is plotted for increasing values of the applied electrostatic field. A complete spatial splitting of the light beam can be achieved at the output of the waveguide. It is worth noting that the numerical curves (Fig.8a) are very similar to the curves in Fig.7c referring

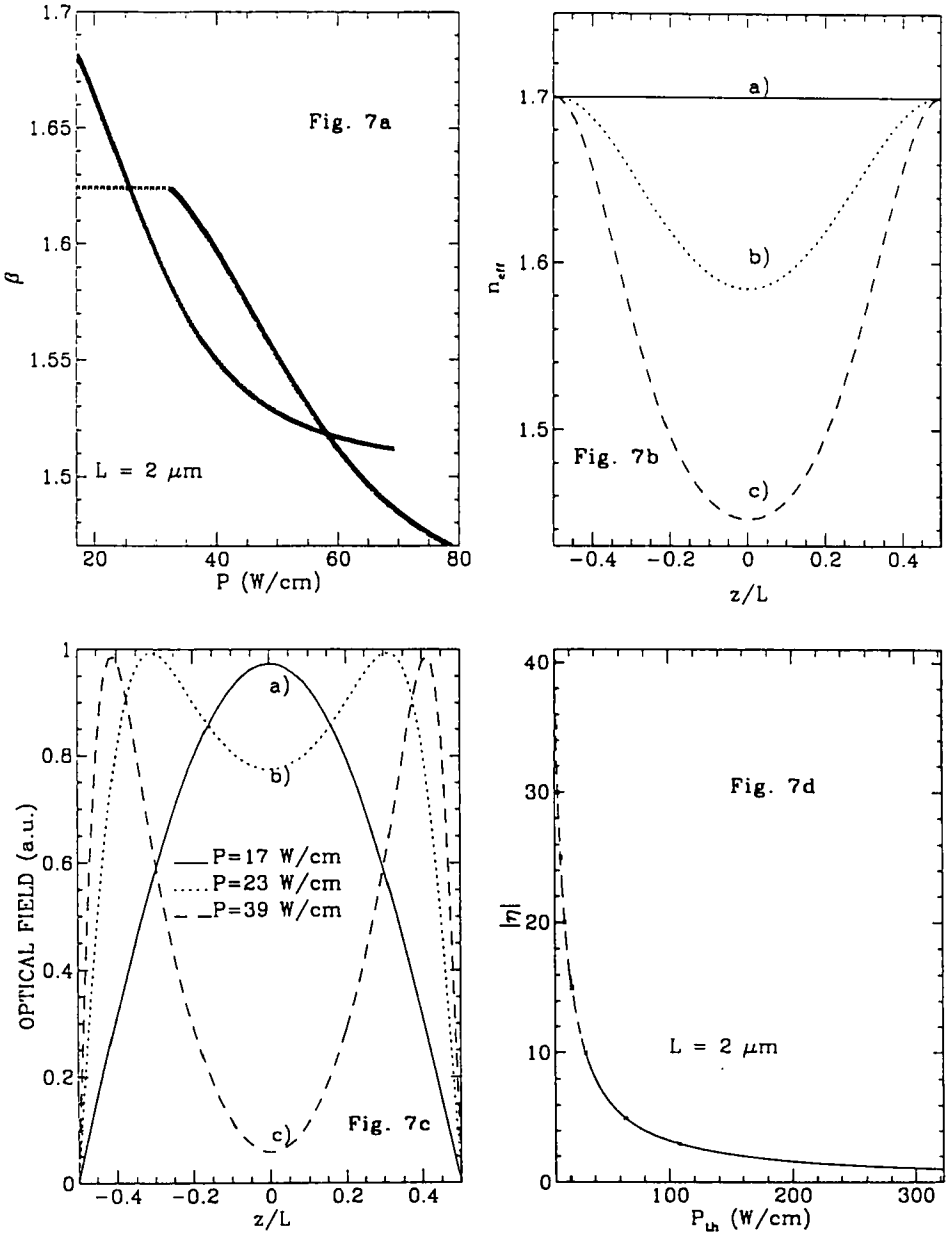

FIGURE 7 Numerical results for a TM-wave in an omeotropical aligned dye-doped LCWG. The propagation constant for the first two modes vs. the power per unit length (7a). The spatial distribution of the effective index (7b) and the field amplitude (7c) for different guided powers. The threshold power vs. the torque amplification factor η.

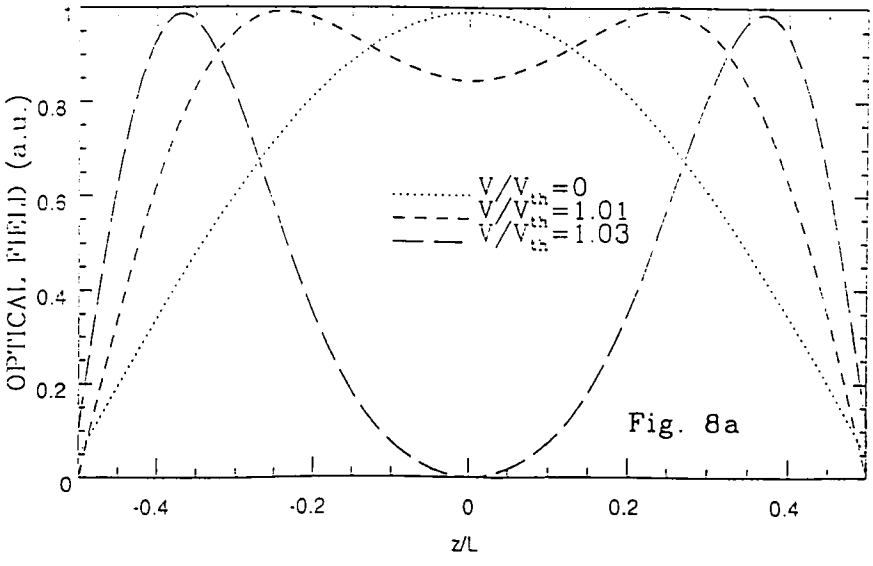

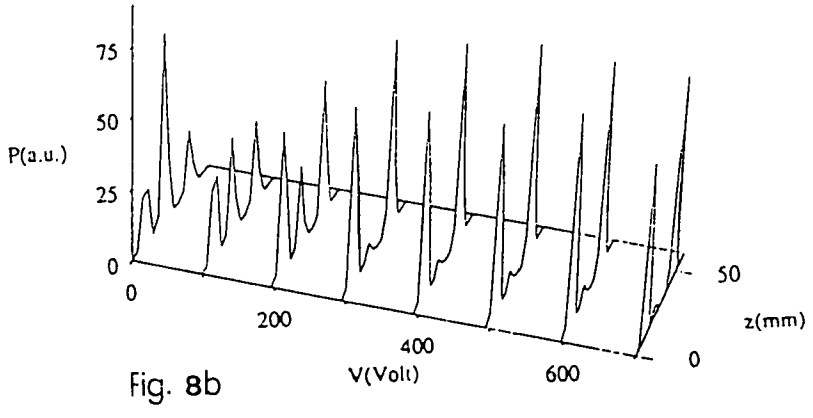

FIGURE 8 Numerical (8a) and experimental (8b) results for a linear TE-wave propagation in a planarly aligned LCWG in the presence of a static electric field: spatial distribution of the optical field for different static electric fields.

to the nonlinear case, apart from the driving field in the abscissa. These seem to us promising results for the realization of the nonlinear device.

CONCLUSION

We have analyzed the nonlinear behavior of planar optical waveguides with liquid crystalline material as a core. We used a plane-wave model for such structures accounting simultaneously for optical field and the material response. With an expressly implemented technique, we solved numerically the model for TM wave propagation in a number of different geometries. We realized a special guiding structure to perform the experiments relative to some of the studied geometries. The results for an HAN configuration are in good agreement with the experimental data. For a planar cell configuration we expect a power threshold for the nonlinear behavior and after that a bistability loop. Till now we have experimentally observed the occurrence of the threshold. The experiment on the bistability is still on way. Finally, in a homeotropic configuration with dye-enhanced negative optical torque, we expect to observe a spatial splitting of the light beam in analogy with what observed with a similar electro-optical liquid crystal device. In the future, we are planning to extend our theoretical, numerical and experimental techniques so that they could be exploited also to study LC cylindrical optical fibers, thus enlarging our understanding of LC guiding devices and their possible applications.

ACKNOWLEDGEMENTS

This work was supported by the European Network LC-MACRONET, by the Italian CNR (Consiglio Nazionale delle Ricerche) and INFM (Istituto Nazionale di Fisica della Materia).

REFERENCES

1. D. J. Channin, Applied Phys. Letters, 22, 365 (1973).
2. C. Hu, J. R. Whinnery, IEEE Journal of Quantum Electronics, QE-10, 556 (1974).
3. N. A. Clark, M. A. Handschy, Applied Phys., 37, 1852 (1990).
4. I. C. Khoo, Hong Li, P. G. LoPresti, Yu Liang, Optics Letters, 19, 530 (1994).
5. G. Abbate, L. De Stefano, P. Mormile, G. Pierattini, E. Santamato, M. Villiargio, Mol. Cryst. Liq. Cryst., 251, 93 (1994).
6. G. Abbate, E. Santamato, L. De Stefano, P. Mormile, G. Pierattini, Optics Comm., 97, 173 (1993)
7. H. Lin, P. Palffy-Muhoray, Optics Letters, 19, 436 (1994).
8. G. Abbate, P. Maddalena, L. Marrucci, E. Santamato, Physical Review E, in press (1995).
9. R. Seydel, Int. J. Bif. and Chaos, 1, 3 (1991).
10. J.Linares, G.C.Righini and J.E.Alvarellos, Applied Optics, 31, 1 (1992)
11. G.Abbate, L.De Stefano, E.Santamato, submitted to JOSA B
12. I. Jánossy, A.D. Lloyd, B.S. Wherrett, Mol.Cryst. Liq. Cryst., 179, (1990).
13. D. Paparo, P. Maddalena, G. Abbate, E. Santamato, I. Jánossy, Mol. Cryst. Liq. Cryst., 251, (1993).
14. G. Abbate, L. De Stefano, P. Mormile, G. Pierattini, E. Santamato, M. Villiargio, Optics Comm., 109, 253 (1994).